Precise Orientation of a Single C_{60} Molecule on the Tip of a Scanning Probe Microscope

C. Chiutu,[1] A. M. Sweetman,[1] A. J. Lakin,[1] A. Stannard,[1] S. Jarvis,[1] L. Kantorovich,[2] J. L. Dunn,[1] and P. Moriarty[1,*]

[1]*School of Physics and Astronomy, University of Nottingham, Nottingham NG7 2RD, United Kingdom*
[2]*Department of Physics, King's College London, The Strand, London, WC2R 2LS, United Kingdom*

(Received 21 November 2011; published 26 June 2012)

We show that the precise orientation of a C_{60} molecule which terminates the tip of a scanning probe microscope can be determined with atomic precision from submolecular contrast images of the fullerene cage. A comparison of experimental scanning tunneling microscopy data with images simulated using computationally inexpensive Hückel theory provides a robust method of identifying molecular rotation and tilt at the end of the probe microscope tip. Noncontact atomic force microscopy resolves the atoms of the C_{60} cage closest to the surface for a range of molecular orientations at tip-sample separations where the molecule-substrate interaction potential is weakly attractive. Measurements of the C_{60}—C_{60} pair potential acquired using a fullerene-terminated tip are in excellent agreement with theoretical predictions based on a pairwise summation of the van der Waals interactions between C atoms in each cage, i.e., the Girifalco potential [L. Girifalco, J. Phys. Chem. **95**, 5370 (1991)].

DOI: 10.1103/PhysRevLett.108.268302 PACS numbers: 82.37.Gk, 31.15.xr, 68.37.Ps, 81.05.ub

Tip functionalization via the controlled transfer of an adsorbed species from a substrate has played a central role in recent remarkable advances in submolecular resolution scanning probe microscopy. In a series of pioneering experiments, Gross and coworkers [1,2] have shown that a CO-functionalized dynamic force microscope tip could be used to image the internal atomic structure of organic molecules with unprecedented resolution. This experimental strategy was subsequently extended to enable quantitative measurements of the intermolecular potential for two CO molecules [3] where a striking agreement between the experimental data and the attractive regime of the theoretical potential for two isolated CO molecules was observed.

Despite these advances, however, the orientation of the tip-adsorbed molecule responsible for submolecular contrast has yet to be directly observed in a dynamic force microscopy experiment. Although important scanning tunneling microscopy (STM) experiments by Schull *et al.* [4] have exploited "reverse imaging" of a tip-adsorbed C_{60} molecule by Cu clusters to ascertain that a hexagonal face of the fullerene was exposed to a Cu(111) surface, selection of different orientational states was not reported, nor was atomic resolution imaging achieved (because STM generally yields a spatial map of the local density of states rather than directly providing atomic resolution, although there are important exceptions [5]). Given that the contrast attained in any scanning probe microscope image is critically dependent on the tip state, and that single-molecule functionalization of the probe will play an increasingly important role in state-of-the-art scanning probe microscope imaging, the development of strategies to determine molecular orientation with the highest possible resolution *at the tip* is essential. We show here that detailed atomic-scale information on the orientation of a single C_{60} molecule adsorbed at the end of a dynamic force microscope tip can be attained directly via submolecular resolution imaging using both (dynamic) STM and atomic resolution frequency-modulation (FM) atomic force microscopy (AFM).

We use a low-temperature ultrahigh vacuum STM-AFM system with tips mounted on tuning fork sensors in the "qPlus" geometry [6] (Omicron Nanotechnology). All images and spectra reported here were acquired at 77 K. The high stiffness of the tuning forks used in our study, $2.6(\pm 0.4)$ kN/m at the position of the tip [7], enables operation with low oscillation amplitudes, increasing sensitivity to short range chemical forces. All FM-AFM measurements are carried out at zero bias. Detailed information on experimental protocols is given in the Supplemental Material [8].

Our approach to imaging, and selecting, the orientation of a tip-adsorbed molecule builds on an elegant experimental protocol pioneered by Giessibl *et al.* [9,10]. This exploits the relatively large separation and narrow spatial extent of the adatom dangling bond orbitals of the Si(111) $-$ (7 $\times$ 7) surface to "reverse image" the tip state [see Fig. 1(a) for schematic illustrations] [11]. Each dangling bond can be considered a "mini-tip" which images the end of the scanning probe because the radius of curvature of the C_{60} molecule is larger than that of the adatom orbitals protruding into the vacuum. Figure 1(b) shows a conventional STM image of the Si(111) $-$ (7 $\times$ 7) surface acquired before the transfer of a C_{60} molecule to the tip. Following the transfer of a C_{60} molecule from the Si(111) $-$ (7 $\times$ 7) surface to the tip [8] [Fig. 1(b)] the adatom features change significantly.

Figures 1(c)–1(e) are direct comparisons between experimental (dynamic) STM data and simulated images calculated on the basis of Hückel molecular orbital theory [12] for three primary orientations of the fullerene cage on

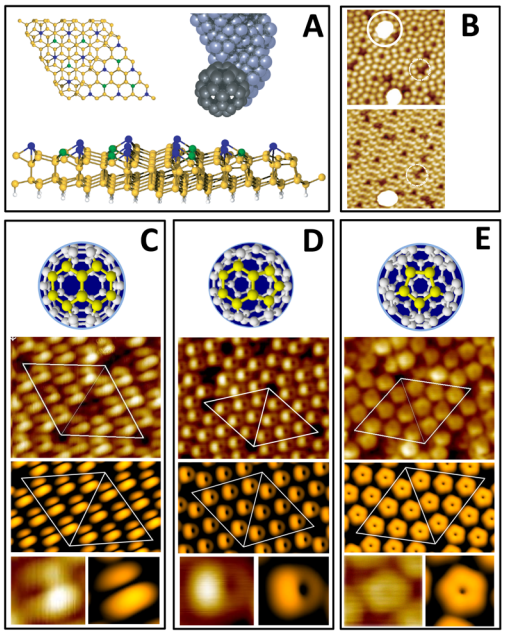

FIG. 1 (color online). Dynamic STM imaging of on-tip C_{60}. (A) Schematic illustrations of the Si(111) − (7 × 7) reconstruction and the experimental tip-sample geometry. (B) STM images acquired before (upper), and after, the transfer of a C_{60} molecule (circled) to the tip. Note the change in the shape of the adatoms following the transfer of the C_{60} molecule. (C) Double-bond-down orientation. The experimental dSTM image [$V = +2.3$ V; $\langle I_t \rangle = 1$ nA; oscillation amplitude $(A_0) = 1.5$ nm] of a silicon adatom (top of frame) comprises two lobes, as predicted by the Hückel theory simulation shown below the experimental data. At the bottom of this frame (and the other frames) we show a direct comparison between a single adatom feature imaged experimentally (left) and the Hückel theory prediction (right). (D) Single-bond-down orientation. dSTM scan parameters: +1 V, 100 pA, $A_0 = 2.25$ Å. (E) Pentagon-down orientation. dSTM scan parameters: +2.3 V, 1 nA, $A_0 = 1.5$ nm.

the tip; namely, double-bond-down, single-bond-down, and pentagon-down. The theoretical STM images have been constructed using Hückel molecular orbitals of C_{60} as an alternative to orbitals from the more widely used density functional theory [8], enabling a computationally inexpensive investigation of a wide range of molecular orientations. Despite the Hückel theory calculations representing a constant current STM image, rather than a constant mean tunnel current ($\langle I_t \rangle$) dynamic STM (dSTM) image, in each case there is excellent qualitative agreement between experiment and theory. (We discuss this distinction between traditional constant current imaging and constant *mean* current feedback in Section III of the Supplemental Material [8]).

Figure 1 illustrates that the orientation of an on-tip C_{60} molecule can be ascertained via a comparison of maps of the local density of states associated with the fullerene molecular orbitals (i.e., STM or dSTM images) with Hückel theory calculations. Although only three primary C_{60} orientations are considered in Fig. 1, both the rotation and tilt of the on-tip fullerene can be ascertained for arbitrary geometries as these directly influence the symmetry of the images [8]. We highlight at this point that while the orientation of a molecule can be adjusted (see, in particular, Fig. S10 of the Supplemental Material [8]), orientational switching at the moment is via a trial-and-error approach.

The ''acid test'' to show that the subatomic features in the images indeed arise from a C_{60} molecule—rather than from, for example, a particular bonding conformation of a silicon atom, dimer, or cluster at the end of the tip [9,10]—is, of course, the observation of structure arising from the fivefold symmetric face of the fullerene cage. The FM-AFM data discussed below provide extremely strong evidence for a ''pentagon-down'' termination of the tip but, as shown in Fig. 1(e), it is also possible to observe the signature of a fivefold symmetric face of the C_{60} cage in STM data. With a pentagon-down orientation the adatom-related features in the experimental dSTM images are typically more radially symmetric with a clear node in the middle. For the highest resolution experimental images [Fig. 1(e)] the type of pentagonal symmetry observed in the Hückel theory simulations for small tip-sample separations becomes evident.

Much higher resolution, down to the atomic level, is possible using frequency modulation dynamic force microscopy (Fig. 2). The origin of atomic-scale resolution for carbon surfaces and nanostructures has, however, been debated intensely. It is only recently that systematic density functional theory calculations (including a semiempirical inclusion of van der Waals interactions) [13] have elucidated the contrast formation mechanism for FM-AFM imaging of these systems. The chemical reactivity of the tip plays a particularly important role. For the C_{60}/Si(111) − (7 × 7) combination used in our experiments, the adatom orbital, by virtue of its partial electron occupation, is a reactive probe of the fullerene and, following both Ondráček *et al.* [13] and Hobbs and Kantorovich [14], we might therefore expect to observe strong contrast at (or close to) the C atom positions in the C_{60} cage.

Figure 2 comprises a set of FM-AFM images of a tip-adsorbed C_{60} molecule in three different orientations. The fivefold symmetric pattern observed at each adatom site in Fig. 2(a) provides compelling evidence that the contrast we observe is indeed due to a C_{60} molecule (rather than a silicon- or contaminant-terminated tip). Not all five atoms of the pentagonal face of the C_{60} molecule are imaged with equal ''intensity'' in the constant frequency shift image. This is because the molecule is tilted slightly, giving rise to a preferential interaction with one of the carbon atoms of the pentagonal face. Despite many repeated attempts with different tips, we did not observe a ''hexagon-down'' orientation during FM-AFM imaging with a C_{60}-terminated tip. We outline possible reasons for this in Section XII of the Supplemental Material [8].

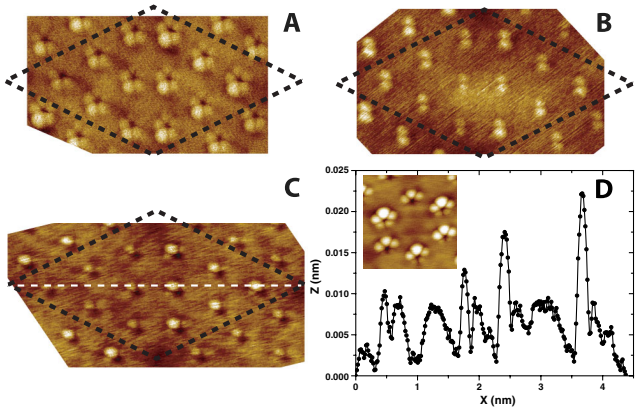

FIG. 2 (color online). Atomic resolution imaging of a single molecule probe. The (7×7) unit cell dimensions are highlighted by dashed lines in (A)–(C). (A) Pentagon-down orientation. (Scan parameters: $A_0 = 2$ Å, Δf set point $= -22.3$ Hz). (B) In this case only two atoms of the fullerene cage are observed—the molecule is oriented such that a single or a double bond is closest to the surface. ($A_0 = 2$ Å, $\Delta f = -46$ Hz). (C) Here there is a larger molecular tilt so that one atom of the C_{60} cage is preferentially imaged. Note also the neighbouring minima (dark "holes" in the image) which arise from the low tip-sample interaction at the centre of the pentagonal and hexagonal faces. ($A_0 = 2$ Å; $\Delta f = -137.4$ Hz). (D) Profile along the dashed line shown in (C). The inset is an FM-AFM image of the same area as (C) but acquired at a higher frequency set point (-150 Hz).

In Fig. 2(b) only two carbon atoms of the C_{60} cage are visible. Ascertaining whether this represents a "single-bond-down" or "double-bond-down" orientation is problematic on the basis of FM-AFM data alone because the separation of the two maxima comprising each adatom feature is 180 pm ± 20 pm—significantly greater than either the C—C or C═C bond length in C_{60}. [As described above, however, (dynamic) STM can be used to determine whether the molecule is in a single-bond-down or double-bond-down state.] One of course would not expect that the "bond length" measured in the FM-AFM image would correspond directly to the accepted values for the C_{60} cage because, as described below, the maxima in the image arise from the chemical interaction of the Si adatoms and the carbon atoms of the fullerene.

Figure 2(c) is an image showing a single strong maximum and only weak subsidary maxima for each adatom feature. At higher frequency set points [see inset to Fig. 2(d)], however, the other atoms of the pentagonal face become visible. It is clear that the molecule is tilted such that one atom of the pentagon is significantly closer to the surface, so as to yield a greater frequency shift. It is also intriguing to note that the Si—C_{60} interaction underpinning the intramolecular atomic contrast is sensitive to the slight difference in electronic structure and chemical reactivity between the faulted and unfaulted halves of the (7×7) unit cell [15], as shown in the line profile of Fig. 2(d).

In order to elucidate the origin of the intramolecular atomic contrast observed in the images of Fig. 2 we have extracted force-distance [$F(z)$] curves from measurements of the change in frequency shift, Δf, of the qPlus sensor as a function of displacement of the tip (Fig. 3). To remove the long range van der Waals and electrostatic contributions to the tip-sample interaction we have adopted the procedure introduced by Lantz *et al.* [16]. In this approach, spectra taken at the centre of a corner hole, which have a negligible short-range chemical force contribution, are used to determine the background $\Delta f(z)$ spectrum. Following extraction of the short range $\Delta f(z)$ curve we use the Sader-Jarvis method [17] to invert the frequency shift measurements to force data.

Figure 3 shows an $F(z)$ curve determined using this procedure for one of the intramolecular maxima in the "pentagon-down" orientation of Fig. 2(a). The first important piece of information to be gleaned from the short range C_{60}—Si $F(z)$ curve is that the maximum attractive force is 1.6(±0.3) nN. This far exceeds what one would expect for a (short range) van der Waals interaction [13] but is entirely consistent with a covalent, or, more accurately, ionocovalent [18], interaction between a silicon adatom and a carbon atom of the C_{60} cage. In addition, there is a clear, and highly reproducible (from sensor to sensor), jump ("discontinuity") in the tip-sample force below a threshold displacement. As discussed below, the origin of this discontinuity becomes clear when the experimental data are compared to the results of density functional theory (DFT) calculations.

We have used an *ab initio* DFT method as implemented in the SIESTA code [19]. Double-zeta polarized basis sets and norm-conserving pseudopotentials were used to describe the atoms within the simulated system and calculations were performed within the generalized gradient approximation Perdew-Burke-Ernzerhof density functional approximation. Typically, atomic relaxation was considered complete when forces on atoms were not larger than 0.01 eV/Å. Due to the size of the calculations only the Γ point was employed in sampling the Brillouin zone for all of our simulations.

An $F(z)$ curve calculated using DFT for a simple model of the C_{60}-adatom interaction is shown alongside the experimental force curve in Fig. 3. Here we have used a simulated cluster which is terminated in a single Si atom back-bonded to three nearest neighbours so as to produce a dangling bond orbital geometry which mirrors that at the (7×7) adatom site. We find that this cluster represents a very good approximation to an adatom in the (7×7) unit cell [8]. The maximum attractive force predicted by the DFT calculations for a pentagon-down geometry is 1.4 nN, in excellent agreement with the experimental data. Equally importantly, the DFT calculations show that the driving force for Si—C bond formation is extremely strong, leading to significant distortions in the C_{60} cage. The Si—C

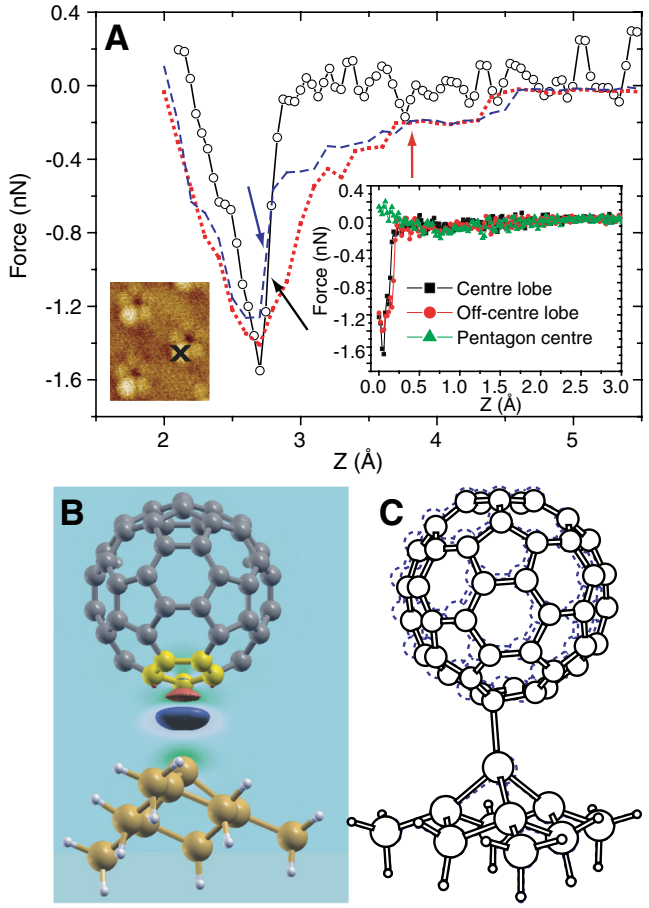

FIG. 3 (color online). Measuring and calculating the chemical force responsible for submolecular atomic contrast. (A) A comparison of an experimentally determined $F(z)$ curve (open circles) with force-displacement relationships calculated using DFT calculations for a silicon adatom directly below a carbon atom (dotted line) and a C—C single bond (dashed line). The arrows highlight a "jump-to-contact" event in the experimental and theoretical data, respectively. Insets: *Left*: Small section of Fig. 2(a) showing position of experimental spectrum in main figure. *Right*: Experimental $F(z)$ curves determined with a different tip and sensor for measurements above the primary maximum (squares) and a secondary lobe (circles) of a pentagonal adatom feature. We also include in the inset the $F(z)$ spectrum for a site at the center of the pentagonal face showing only a very weak attractive interaction before the repulsive regime of the C_{60}—Si potential is entered. (B) A charge density difference plot showing the formation of a Si—C bond at a tip-sample separation of 3.8 Å (see also Ref. [8]). [This separation is highlighted with an arrow in (A)]. The red contours represent a charge density difference of -0.005 Å^3 (density depletion) and the blue contours a difference of $+0.005$ Å^3 (density excess). (C) A cartoon representation of the distortion of the C_{60} cage induced via the formation of a bond with a silicon adatom. The solid line represents the carbon atom and bond positions for the molecule at a position before the sharp jump in $F(z)$ [marked by the blue arrow in (A)]; the dotted lines represent the corresponding positions immediately after the jump in $F(z)$, corresponding to a C_{60} position 0.1 Å closer to the adatom.

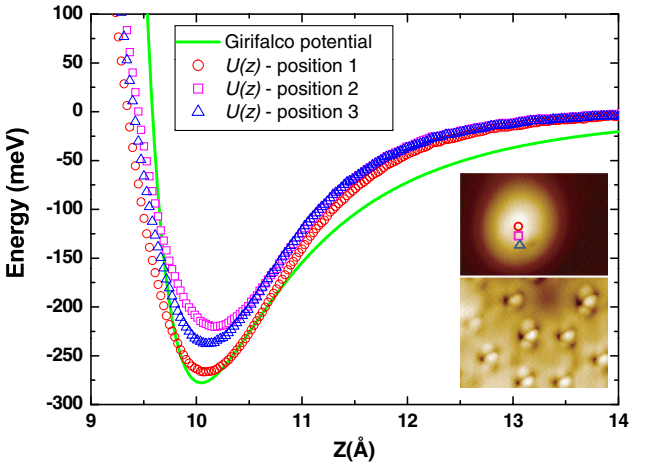

FIG. 4 (color online). Determining the C_{60}—C_{60} pair potential. After confirming the C_{60} termination of the tip (lower inset, FM-AFM image with $A_0 = 2$ Å and $\Delta f = -43$ Hz), a buckminsterfullerene molecule adsorbed on the Si(111) $-$ (7 $\times$ 7) surface was located (upper inset, $\Delta f = -18.5$ Hz) and $\Delta f(z)$ spectra measured at the positions shown in the upper inset. From these measurements we extracted the C_{60} pair potential at various positions on the surface-adsorbed molecule. For comparison we have also plotted the analytical Girifalco potential for the C_{60}—C_{60} intermolecular interaction (solid line) with no adjustment or fitting other than an alignment of the minima of the experimental and theoretical curves.

interaction produces an effective "snap-to-contact" for a variety of orientations of the on-tip C_{60}, an example of which is highlighted by the blue arrow in Fig. 3. This type of sharp jump in the $F(z)$ curve is also repeatedly observed in experiment (black arrow in Fig. 3). That the tip-sample interaction is underpinned by Si—C bond formation is highlighted even further by the density difference plot shown in Fig. 3(b) while Fig. 3(c) illustrates the extent to which the fullerene cage is distorted due to the change in hybridization of the C atom involved in bonding to the underlying Si adatom.

The ability to image—and, indeed, switch [8]—the orientation of a single molecule terminating a scanning probe enables the direct measurement of interfullerene interactions (Fig. 4). Up to this point we have considered the C_{60}-on-Si system; we now move to address the interaction of the on-tip C_{60} molecule with a surface-adsorbed molecule. We have first ascertained the orientation of the tip-adsorbed C_{60} molecule (lower inset to Fig. 4) via the adatom "inverse imaging" technique described above. A C_{60} molecule on the Si(111) $-$ (7 $\times$ 7) surface was subsequently located (upper inset to Fig. 4) and $\Delta f(z)$ spectroscopy measurements made at a number of positions on the molecule. In Fig. 4 we show a number of the $U(z)$ curves extracted from these $\Delta f(z)$ data [8], alongside the most frequently used model pair potential for C_{60}—C_{60} interactions, derived by Girifalco [20].

The analytical Girifalco potential has been compared to the results of DFT calculations [21] and has been shown to provide an excellent description of C_{60} interactions. Our experimentally determined C_{60} pair potential [8] is in very good agreement with the Girifalco model, particularly given the experimental uncertainties and that Girifalco's potential cannot account for relaxation of the molecule on the tip (or surface) nor for the presence of dipoles or variations in polarizability due to adsorption on the tip or surface. The relaxation of the C_{60} molecules leads to a shallower gradient in the repulsive regime of the intermolecular potential than that predicted by the Girifalco potential. A similar reduction in gradient was observed for both C_{60}—Cu [22] and CO—CO [3] interactions.

Small changes in the position of the probe molecule (see inset to Fig. 4) produce reproducible variations in both the profile of the intermolecular potential and the depth of the well. The intermolecular binding energy predicted by the Girifalco potential exclusively arises from *short range* dispersion forces. Nonetheless, the magnitude of the variation we observe (~ 50 meV) is in line with that predicted by the DFT calculations of Tournus, Charlier, and Mélinon [23] using the local density approximation and taking no account of van der Waals forces. Hexagon-hexagon vs pentagon-pentagon (or hexagon-pentagon) interactions give rise to different intermolecular binding energies due to the difference in the electron density for the 6:6 and 5:6 bonds in the fullerene cage. The spatial variation of the pair potentials extracted from our data reflect this intramolecular modulation of the electron density.

Direct atomic resolution imaging of the orientation of a molecule at the end of a tip facilitates a variety of exciting ''next generation'' scanning probe experiments. These include the mapping of the orientational dependence of intermolecular force fields and interaction potentials, and the analysis of the influence of the ''rotational probe state'' on molecular manipulation. The ability to control on-tip molecular orientation will be of especial value for the analysis and manipulation of systems exhibiting *anisotropic* force fields, including, in particular, hydrogen-bonded assemblies [24].

P. M. and A. S. thank the Engineering and Physical Sciences Research Council (EPSRC) and the Leverhulme Trust, respectively, for Grants [No. EP/G007837/1, and No. ECF/2010/0380]. A. M. S. acknowledges funding from the Leverhulme Trust [Grant No. F00/114 BI]. C. C. is grateful for a Marie Curie fellowship funded by the NANOCAGE FP6 training network. S. J. and A. J. L. are funded through EPSRC doctoral training accounts. We also acknowledge the support of the University of Nottingham High Performance Computing Facility (in particular, Dr. Colin Bannister). Juergen Koeble and Andreas Bettac of Omicron Nanotechnology GmbH provided advice and assistance with regard to our qPlus AFM system. C. C., S. J., A. J. L., A. S., and A. M. S. contributed equally to this work.

*Corresponding author.
philip.moriarty@nottingham.ac.uk

[1] L. Gross, F. Mohn, N. Moll, P. Liljeroth, and G. Meyer, Science **325**, 1110 (2009).
[2] L. Gross, F. Mohn, N. Moll, G. Meyer, R. Ebel, W. Abdel-Mageed, and M. Jaspars, Nature Chem. **2**, 821 (2010).
[3] Z. Sun, M. P. Boneschanscher, I. Swart, D. Vanmaekelbergh, and P. Liljeroth, Phys. Rev. Lett. **106**, 046104 (2011).
[4] G. Schull, Y. Dappe, C. González, H. Hulou, and R. Berndt, Nano Lett. **11**, 3142 (2011).
[5] C. Weiss, C. Wagner, C. Kleimann, M. Rohlfing, F. S. Tautz, and R. Termirov, Phys. Rev. Lett. **105**, 086103 (2010).
[6] F. Giessibl, Appl. Phys. Lett. **76**, 1470 (2000).
[7] A. Sweetman, S. Jarvis, R. Danza, J. Bamidele, S. Gangopadhyay, G. A. Shaw, L. Kantorovich, and P. Moriarty, Phys. Rev. Lett. **106**, 136101 (2011).
[8] See Supplemental Material at http://link.aps.org/supplemental/10.1103/PhysRevLett.108.268302 for full details of the experimental and theoretical protocols, a detailed discussion of the analysis of molecular orientation and tilt, and a number of additional experimental results related to orientational switching and the measurement of intermolecular potentials.
[9] F. Giessibl, S. Hembacher, H. Bielefeldt, and J. Mannhart, Science **289**, 422 (2000).
[10] M. Herz, F. J. Giessibl, and J. Mannhart, Phys. Rev. B **68**, 045301 (2003).
[11] A. Campbellová, M. Ondrácek, P. Pou, R. Pérez, P. Klapetek, and P. Jelínek, Nanotechnology **22**, 295710 (2011).
[12] I. D. Hands, J. L. Dunn, and C. A. Bates, Phys. Rev. B **81**, 205440 (2010).
[13] M. Ondráček, P. Pou, V. Rozsival, C. Gonzalez, P. Jelinek, and R. Perez, Phys. Rev. Lett. **106**, 176101 (2011).
[14] C. Hobbs and L. Kantorovich, Surf. Sci. **600**, 551 (2006).
[15] M. Abe, Y. Sugimoto, O. Custance, and S. Morita, Appl. Phys. Lett. **87**, 173503 (2005).
[16] M. Lantz, H. Hug, R. Hoffmann, P. van Schendel, P. Kappenberger, S. Martin, A. Baratoff, and H. Guntherodt, Science **291**, 2580 (2001).
[17] J. Sader and S. Jarvis, Appl. Phys. Lett. **84**, 1801 (2004).
[18] B. Masenelli, F. Tournus, P. Melinon, X. Blase, A. Perez, M. Pellarin, M. Broyer, A. Flank, and P. Lagarde, Surf. Sci. **532-535**, 875 (2003).
[19] J. M. Soler, E. Artacho, J. D. Gale, A. García, J. Junquera, P. Ordejón and D. Sánchez-Portal, J. Phys. Condens. Matter **14**, 2745 (2002).
[20] L. Girifalco, J. Phys. Chem. **95**, 5370 (1991).
[21] J. M. Pacheco and J. P. Prates Ramalho, Phys. Rev. Lett. **79**, 3873 (1997).
[22] R. Pawlak, S. Kawai, S. Fremy, T. Glatzel, and E. Meyer, ACS Nano **5**, 6349 (2011).
[23] F. Tournus, J.-C. Charlier, and P. Mélinon, J. Chem. Phys. **122**, 094315 (2005).
[24] J. Theobald, N. Oxtoby, M. Phillips, N. Champness, and P. Beton, Nature (London) **424**, 1029 (2003).